BRITISH ECOLOGICAL SOCIETY Functional Ecology

The negative effects of an allelopathic invader on native plant photosynthesis are observed after tree canopy closure

Journal:	*Functional Ecology*
Manuscript ID	FE-2025-01432
Wiley - Manuscript type:	Research Article
Key-words:	Alliaria petiolata, AM fungi, plant invasion, stomatal conductance, J_{max}, V_{max}, symbiosis

"The negative effects of an allelopathic invader on native plant photosynthesis are observed after tree canopy closure"

Abstract

1. Many invasive plants produce allelopathic compounds that disrupt plant-fungal symbioses of native species in the communities they invade, influencing nutrient and water provisioning to support photosynthesis. Previous studies have linked these disruptions to reductions in photosynthesis and stomatal conductance, but whether these effects are tied to reductions in photosynthetic capacity remain unclear, limiting inferences about the mechanisms driving physiological responses of native species. Furthermore, how these responses vary temporally across the growing season is unknown.
2. To investigate the temporal dynamics of native plant responses to allelopathic invasion, we measured gas exchange in two understory native species (*Trillium* spp. and *Maianthemum racemosum*) at two points during the growing season – before and after tree canopy closure. Plants were measured in a long-term field experiment where *Alliaria petiolata*, an allelopathic invader that disrupts AM fungal symbioses, has been removed or left at ambient levels since 2006.
3. Both native species exhibited significantly reduced net photosynthesis rates under ambient *A. petiolata* levels compared to the weeded treatment. This response was due to a reduction in apparent photosynthetic capacity in *Trillium* spp. and a reduction in stomatal conductance that increased stomatal limitation in *M. racemosum*. Photosynthetic responses to *A. petiolata* in both species were only observed after tree canopy closure.
4. Our findings indicate that *A. petiolata* reduces native plant net photosynthesis either by increasing nutrient stress, as indicated by the reduction in apparent photosynthetic capacity (*Trillium* spp.), or by increasing water stress, as indicated by the reduction in stomatal conductance (*M. racemosum*), and that these responses only become apparent after the tree canopy closed. These results highlight the importance of seasonal changes that can regulate plant physiological responses to allelopathic invaders and demonstrate the diversity of mechanisms by which allelopathic invaders can influence native plant physiology.

Keywords
Alliaria petiolata, AM fungi, photosynthesis, plant invasion, symbiosis, stomatal conductance, V_{cmax}, J_{max}

Introduction

Invasive plants often express unique traits that increase their likelihood of establishment in novel ecosystems. Allelopathy, defined as a secondary compound produced by a plant that negatively impacts neighboring plant species and/or soil microbial communities (Inderjit et al., 2011), has emerged as a mechanism to explain the success of some invasive plant species (Callaway et al., 2008; Callaway & Ridenour, 2004). Allelopathy is estimated to occur in 52% of invasive plant species (Kalisz et al., 2021) and has been shown to negatively affect native plant performance and soil microbial community composition in both field and greenhouse settings (Bialic-Murphy et al., 2020, 2021; Brouwer et al., 2015; Hale et al., 2011, 2016; Hale & Kalisz, 2012; Qu et al., 2021; Roche et al., 2021; Zhang et al., 2021). Despite the prevalence of allelopathy among invasive species, our understanding of the mechanisms that drive the physiological responses of native species to allelopathic invasion and the temporal dynamics that underpin these responses remains limited. This knowledge gap hinders our understanding of how the disruptive impacts of allelopathic invasion on soil microbial communities scale to influence plant community dynamics.

Photosynthesis links ecosystem carbon, nutrient, and water cycles in terrestrial ecosystems (Hungate et al., 2003). Through photosynthesis, plants convert carbon dioxide into simple sugars using enzymes such as Ribulose-1,5-bisphosphate (RuBP) carboxylase/oxygenase (Rubisco). These enzymes require high amounts of nutrients and energy to build and maintain, creating a large nutrient and energy demand for the plant (Evans & Clarke, 2019; Evans & Seemann, 1989). Photosynthetic capacity, or the biochemical capacity at which a leaf can fix carbon, can be estimated from the maximum rate of Rubisco carboxylation (V_{cmax}), standardized to a common temperature (e.g., 25°C; V_{cmax25}) and the maximum rate of electron transport for RuBP regeneration (J_{max}), standardized to a common temperature (e.g., 25°C; J_{max25}) (Ali et al., 2015; Farquhar et al., 1980). V_{cmax} and J_{max} are often positively correlated with leaf nitrogen and phosphorus content and are commonly used as physiological indicators of nutrient stress

(Ellsworth et al., 2022; Evans, 1989; Walker et al., 2014). Photosynthesis is also regulated by stomatal conductance, which controls CO_2 diffusion into the leaf and supports transpiration (Farquhar & Sharkey, 1982). Transpiration allows for the uptake and transport of water and nutrients by the roots through the plant vascular system to photosynthetic tissues. Stomates close and stomatal conductance generally declines with increasing water limitation, making it a useful physiological indicator of water stress (Medrano et al., 2002). Because leaf-level photosynthesis reflects photosynthetic capacity and stomatal conductance, assessing how both respond individually to allelopathic invaders can clarify the physiological mechanisms that drive native species responses.

Allelopathic compounds with antimicrobial properties can inhibit the growth and reproduction of soil microbial communities, such as mycorrhizal fungi, which are essential for plant nutrient and water uptake (Hale & Kalisz, 2012). Arbuscular mycorrhizal (AM) fungi often form obligate symbioses with plants, exchanging mineral nutrients and water for photosynthate (S. E. Smith & Read, 2008). Antimicrobial compounds produced by allelopathic invaders can disrupt these symbioses by inhibiting AM fungal spore germination, fungal root colonization, and arbuscule formation, which can decrease AM fungal biomass in roots and soil, alter AM fungal species richness, and modify AM fungal community composition (Burke, 2008; Callaway et al., 2008; Burke et al., 2011; Cantor et al., 2011; Anthony et al., 2019; Bialic-Murphy et al., 2021). These disruptions may decrease nutrient and water uptake in plants that rely on AM fungi, even when allelopathic invaders do not directly modify ecosystem nutrient or water availability (Bialic-Murphy et al., 2021). Disruptions in AM fungal mutualisms may increase the plant carbon cost for acquiring nutrients and water, causing plants to receive less resources provisioned by AM fungal partners for a given belowground carbon investment (Hale et al., 2016; Kummel & Salant, 2006). This pattern may scale to alter resource allocation to photosynthetic enzymes, as emerging evidence suggests that increased costs of nutrient acquisition are associated with altered nutrient allocation to photosynthetic enzymes (Perkowski et al., 2021, 2025; Waring et al., 2023). Thus, all else being equal (e.g., competition for soil resources), disruptions in AM fungal mutualisms due to allelopathy could cause native plants to be unable to satisfy the demand to build and maintain photosynthetic enzymes and/or maintain stomatal conductance, which may explain why native species exhibit reduced net photosynthesis

rates and consequent fitness declines in response to allelopathic invaders (Bialic-Murphy et al., 2020; Hale et al., 2011, 2016).

Alliaria petiolata (M. Bieb) Cavara & Grande (Family: Brassicaceae) is a model species for investigating the impacts of allelopathic plant invasion on native plant communities. This biennial herb from Eurasia invades temperate forest understories in North America and releases glucosinolates into soil environments through root exudation and leaf litter (Rodgers et al., 2008). Glucosinolates produced by *A. petiolata* hydrolyze into antimicrobial compounds such as allyl isothiocyanate that inhibit AM spore germination, spore viability, root colonization, and arbuscule formation (Anthony et al., 2019; Callaway et al., 2008; Cantor et al., 2011). Field studies show that *A. petiolata* invasion reduces AM fungal biomass, increases AM species richness, and alters fungal community composition (Table 1; Bialic-Murphy et al., 2021; Burke, 2008; Burke et al., 2011; Cantor et al., 2011). These AM fungal community changes are associated with negative impacts on native plant nutrient and water economics, population dynamics, and community composition (Bialic-Murphy et al., 2020, 2021; Hale et al., 2016; Roche et al., 2021, 2023), with stronger negative impacts in native species that associate with AM fungi compared to those that are non-mycorrhizal (Callaway et al., 2008; Roche et al., 2021, 2023). These patterns occur despite evidence that *A. petiolata* invasions do not affect soil nutrient or water availability, suggesting that the breakdown of the AM fungal mutualism is the mechanism that drives native plant community responses to *A. petiolata* (Bialic-Murphy et al., 2021; Burke et al., 2019).

Previous work also indicates that *A. petiolata* reduces net photosynthesis in a common forest understory native, *M. racemosum*, through a reduction in stomatal conductance (Brouwer et al., 2015; Hale et al., 2011, 2016). However, the mechanisms that regulate these responses are not fully understood, in part because the concurrent photosynthetic capacity responses (i.e., V_{cmax}, J_{max}) of native species growing with *A. petiolata* have not been quantified. Photosynthetic responses of native species to *A. petiolata* presence could be driven by changes in photosynthetic capacity, indicating nutrient limitation, or by changes in stomatal conductance, indicating water limitation. Understanding whether changes in photosynthetic capacity or stomatal conductance drive such photosynthetic responses to *A. petiolata* presence would provide valuable insight into the underlying mechanism. Furthermore, existing field research has quantified photosynthetic responses to *A. petiolata* presence at a single time point in the growing season, providing limited

insight into the extent to which the impacts of *A. petiolata* change across the growth season as understory light availability and soil resource availability decrease. For example, high light availability due to an open tree canopy early in the growing season should increase demand to build and maintain photosynthetic enzymes in the understory. This, in turn, could magnify the effects of disrupted AM fungal communities on native plants' resource uptake and allocation to photosynthetic tissues. Alternatively, reductions in soil resource availability later in the growing season could increase reliance on disrupted AM fungal communities by native plant physiology, thereby exacerbating the effects of disrupted AM fungal communities on investment in photosynthesis. Measurements at different time points in the growing season are needed to assess the relative magnitude of leaf-level physiological responses to allelopathic invaders and how this relates to the fine-scale impacts on AM fungal community composition and the broad-scale effects on native plant productivity and survivorship.

Here, we assessed the temporal dynamics that drive the effects of allelopathic invasion on leaf-level photosynthetic processes of two coexisting native plant species growing with and without the presence of *A. petiolata*. To do this, we collected gas exchange measurements at two measurement timepoints (open canopy early in growing season, closed canopy later in the growing season) from two understory native species (*Trillium* spp. and *Maianthemum racemosum*) in a long-term *A. petiolata* field manipulation experiment. We used these measurements and experimental setup to assess the following hypotheses:

1) Both native species will experience reduced net photosynthesis in the *A. petiolata*-ambient treatment compared to the *A. petiolata*-weeded treatment. These patterns will be associated with reduced temperature-standardized apparent photosynthetic capacity (i.e., V_{cmax25}, J_{max25}), relative chlorophyll content, and stomatal conductance, in the *A. petiolata*-ambient treatment. We expected that a reduction in apparent photosynthetic capacity and/or relative chlorophyll content in response to *A. petiolata* presence would indicate nutrient stress, while a reduction in stomatal conductance and increase in stomatal limitation would indicate water stress.
2) The negative effects of *A. petiolata* on the photosynthetic traits of native species will depend on time in the growing season.
    a) The negative effects of *A. petiolata* treatment on leaf photosynthetic traits will be greatest early in the growing season when photosynthetic demand for soil

resources is highest (i.e., due to increased understory light availability). Disrupted AM fungal symbioses will create resource stress, making it more difficult for AM-associating plants to acquire nutrients and water needed to satisfy photosynthetic demand for soil resources.

b) Alternatively, the negative effects of *A. petiolata* treatment on photosynthetic traits will be greatest later in the growing season. This response may be driven by increased reliance on disrupted AM fungal partners for soil nutrients and water as resources are depleted. However, as tree canopy closure reduces light availability, photosynthetic demand for soil resources may also decline, which may mitigate the effects of AM fungal disruption on late-season physiology.

Table 1 Relative effects of *A. petiolata* ambient vs. removal treatments on soil, AM fungal, native plants, native community metrics in a long-term (2006-2025) experiment at Trillium Trail Reserve, Fox Chapel, PA.

Metric Category	Metric	*A. petiolata* effect	Evidence	Citation
Soil characteristics	Soil moisture	No change	No difference between *A. petiolata*-ambient and weeded plots	(Bialic-Murphy et al., 2021; Burke et al., 2019)
	Soil nutrient availability	No change	No difference between *A. petiolata*-ambient and weeded plots	(Bialic-Murphy et al., 2021; Burke et al., 2019)
	Soil carbon	+	Soil C is greater in *A. petiolata*-weeded plots	(Burke et al., 2019)
AM fungal community composition and function	AM fungal spore germination	-	Reduced spore germination by *A. petiolata* allelochemicals	(Cantor et al., 2011)
	AM fungal colonization in roots	-	Higher colonization in *A. petiolata*-weeded treatment	(Mutz et al. in review; Bialic-Murphy et al., 2021)
	Soil AM fungal hyphal lengths	-	Lower fungal hyphal lengths in *A. petiolata*-ambient plots	(Cantor et al., 2011; Hale et al., 2016)
	AM fungal spore abundance in soil	No change	No change	(Burke et al., 2019)
	AM fungal diversity (richness) in soil	No change	No change	(Bialic-Murphy et al., 2021)
	AM fungal diversity (richness) in roots	No change	No change	(Mutz et al. in review)
	AM fungal community composition in soil	Change	AM fungal composition shift in mineral soil	(Bialic-Murphy et al., 2021; Burke, 2008; Burke et al., 2011, 2019)
	AM fungal community composition in native plant roots	Change	AM fungal composition shift in native plant roots	(Mutz et al. in review)
	Soil nutrient provisioning to native plants ($\delta^{15}N$)	-	Native plant $\delta^{15}N$ higher in *A. petiolata*-invaded plots	(Mutz et al. in review)
Native plant community structure	Mycorrhizal plant abundance	-	Native AM plant abundance decreases with *A. petiolata*	(Roche et al., 2021, 2023)
Native plant physiology and allocation	Stored carbon (inulin) in *Maianthemum*	-	*A. petiolata* leaf litter reduced stored carbon (inulin) in *Maianthemum*	(Hale et al., 2016)
	Soil respiration (microbial activity)	-	*A. petiolata* tissue slowed soil respiration	(Hale et al., 2011)
	Net photosynthesis in *Maianthemum*	-	*A. petiolata* decreases net photosynthesis rates	(Brouwer et al., 2015; Hale et al., 2011)
	Stomatal conductance in *Maianthemum*	-	*A. petiolata* decreases stomatal conductance	(Brouwer et al., 2015; Hale et al., 2011)
	Photosynthetic capacity (V_{cmax}, J_{max})	?	No evidence prior to this study	This study
	Temporal variation across growing season	?	No evidence prior to this study	This study

Materials and Methods

Study site and experimental design

This study was conducted at Trillium Trail Nature Reserve in Fox Chapel, Pennsylvania, USA (40.520 °N, -79.901 °W). The mean annual precipitation of the study area is 1006 mm yr^{-1} and the mean annual temperature is 11°C (2006-2020 U.S. Climate Normals; Palecki et al., 2021). Wire fences (2.5 m tall) were set up in 2002 at five 14 x 14 m experimental plots to exclude deer while allowing free movement of small mammals and birds. *Alliaria petiolata* has been manually weeded at the beginning of each growth season from one half of each experimental plot since 2006, with *A. petiolata* remaining at natural densities in the other half of each plot. Manual weeding has been an effective strategy for *A. petiolata* removal, with relative abundance of *A. petiolata* averaging 0.08% in years that followed the initial weeding treatment in 2006 (Roche et al., 2021). This long-term split-plot experiment is located on 25-75% grade slopes. Soils were classified as Gilpin-Upshur-Atkins soils with dominant shale, sandstone, and red clay shale bedrock components. *Alliaria petiolata* treatments were set up parallel to the slope to prevent allelochemical leaching into the weeded side of the plot. Previous work conducted in this experiment has shown that *A. petiolata*-ambient plots exhibit decreased AM fungal biomass, decreased AM root colonization rates, and increased AM fungal richness compared to *A. petiolata*-weeded plots (Burke, 2008; Burke et al., 2011; Cantor et al., 2011), which has altered the AM fungal community composition between treatments (Bialic-Murphy et al., 2021) (Table 1). Additionally, soil nutrient availability and soil water availability did not differ between *A. petiolata* treatments (Bialic-Murphy et al., 2021; Burke et al., 2019) (Table 1), at a single timepoint.

Gas exchange measurements and calculations

Gas exchange measurements were collected between April and June 2023 from fully expanded leaves of two perennial understory native species: *Trillium* spp. (*Trillium grandiflorum* (Michx.) Salisb and *Trillium erectum* L.) and *Maianthemum racemosum* L. Link. We use *Trillium* spp. to refer to *T. grandiflorum* and *T. erectum*, as these species are difficult to distinguish if they are not reproductive. *Trillium* spp. and *M. racemosum* are understory perennial herbs that form rhizomes (i.e., geophytes), with widespread distributions in temperate forests of North America (USDA

NRCS, 2022). Both species associate with AM fungi (Brundrett & Kendrick, 1987, 1990; Burke, 2008).

Gas exchange data were collected in three of the five experimental plots during two measurement periods: once early in the growth season when the tree canopy was open and tree canopy leaf out was occurring (April 19 through April 21 for *Trillium* spp. and May 5 through May 6 for *M. racemosum*) and once later in the growth season when the tree canopy was fully closed (June 12 through June 15 for both species). The first measurement period was conducted at different time points for *Trillium* spp. and *M. racemosum* because of differences in the timing of full leaf expansion of the two species (Heberling et al., 2019). Two of the five plots were excluded from gas exchange measurements due to an insufficient number of the focal native species within them. Gas exchange data across the three sampled plots allowed us to confidently assess the effects of *A. petiolata* on native plant physiology (n = 32 individuals for *Trillium* spp., 33 individuals for *M. racemosum* Table 2).

Net photosynthesis (A_{net}; μmol m^{-2} s^{-1}), stomatal conductance (g_{sw}; mol m^{-2} s^{-1}), and intercellular CO_2 (C_i; μmol mol^{-1}) concentrations were measured across a range of atmospheric CO_2 concentrations (i.e., an A_{net}/C_i curve) using the Dynamic Assimilation™ Technique (Saathoff & Welles, 2021). This technique allows for high-throughput A_{net}/C_i curves that correspond well with traditional steady-state methods in herbaceous species (Tejera-Nieves et al., 2024). We generated all A_{net}/C_i curves along a reference CO_2 ramp down from 420 μmol mol^{-1} CO_2 to 20 μmol mol^{-1} CO_2, followed by a ramp up from 420 μmol mol^{-1} CO_2 to 1620 μmol mol^{-1} CO_2 after a 90-second wait period at 420 μmol mol^{-1} CO_2. The ramp rate for each curve was set to 200 μmol mol^{-1} min^{-1}, logging every five seconds, which generated 96 data points per response curve. All A_{net}/C_i curves were initiated after A_{net} and g_{sw} stabilized in a LI-6800 cuvette set to a 500 mol s^{-1} flow rate, 10000 rpm mixing fan speed, 1.5 kPa vapor pressure deficit, 25°C leaf temperature, 2000 μmol m^{-2} s^{-1} incoming light radiation, and initial reference CO_2 set to 420 μmol mol^{-1}. We extracted snapshot A_{net} and g_{sw} measurements using the initial measurement of each A_{net}/C_i curve at 420 μmol mol^{-1} CO_2.

A/Ci curve fitting and parameter estimation

We fit A_{net}/C_i curves using the 'fitaci' function in the 'plantecophys' R package (Duursma, 2015). This function estimates the maximum rate of Rubisco carboxylation (V_{cmax}; μmol m^{-2} s^{-1})

and maximum rate of electron transport for RuBP regeneration (J_{max}; μmol m^{-2} s^{-1}) using the Farquhar et al. (1980) biochemical model of C_3 photosynthesis. Restrictions on triose phosphate utilization (TPU) were included as an additional rate-limiting step in all curve fits and the temperature standardization default in the function was turned off. Dark respiration was estimated in each curve fit as a fixed proportion of V_{cmax}. Michaelis-Menten coefficients for Rubisco affinity to CO_2 (K_c; μmol mol^{-1}) and O_2 (K_o; mmol mol^{-1}), and the CO_2 compensation point (Γ^*; μmol mol^{-1}) were calculated using leaf temperature and equations derived in Bernacchi et al. (2001):

$$K_c = 404.9 * exp^{\left(\frac{79430(T_k-298)}{298RT_k}\right)} \quad (1)$$

$$K_o = 278.4 * exp^{\left(\frac{36380(T_k-298)}{298RT_k}\right)} \quad (2)$$

$$\Gamma^* = 42.75 * exp^{\left(\frac{37830(T_k-298)}{298RT_k}\right)} \quad (3)$$

In all three equations, T_k is the mean leaf temperature (in Kelvin) during each A_{net}/C_i curve, and R is the universal gas constant (8.314 J mol^{-1} K^{-1}). All curves were visually inspected for goodness-of-fit before extracting V_{cmax} and J_{max} estimates for hypothesis testing.

For all A_{net}/C_i curve fits, V_{cmax} and J_{max} were standardized to 25°C (referenced as V_{cmax25} and J_{max25}) using a modified Arrhenius equation. This temperature standardization removed the influence of enzyme kinetics on V_{cmax} and J_{max}, and, thus, reflected biochemical investment in the different underlying processes (Atkin & Tjoelker, 2003). Rate estimates were standardized to 25°C using the formulation presented in Kattge and Knorr (2007):

$$k_{25} = \frac{k_{obs}}{e^{\left[\frac{H_a(T_{obs}-T_{ref})}{T_{ref}RT_{obs}}\right]} \times \frac{1+e^{\left(\frac{T_{ref}\Delta S-H_d}{RT_{ref}}\right)}}{1+e^{\left(\frac{T_{obs}\Delta S-H_d}{RT_{obs}}\right)}}} \quad (4)$$

where k_{25} represents the standardized V_{cmax} or J_{max} rate at 25°C, k_{obs} represents the V_{cmax} or J_{max} estimate at the average leaf temperature measured inside the cuvette during the A_{net}/C_i curve. H_a is the activation energy of V_{cmax} (71,513 J mol^{-1}; Kattge and Knorr, 2007) or J_{max} (49,884 J mol^{-1}; Kattge and Knorr, 2007). H_d represents the deactivation energy of both V_{cmax} and J_{max} (200,000 J mol^{-1}; Medlyn et al., 2002), and R represents the universal gas constant (8.314 J mol^{-1} K^{-1}). T_{ref} represents the standardized temperature of 298.15 K, and T_{obs} represents the mean leaf temperature (K) during each A_{net}/C_i curve. ΔS is an entropy term (J mol^{-1} $°C^{-1}$) that Kattge and

Knorr (2007) described as a linear relationship with acclimated growth temperature (T_g, °C), where:

$$\Delta S_{vcmax} = -1.07T_g + 668.39 \quad (5)$$

and:

$$\Delta S_{jmax} = -0.75T_g + 659.70 \quad (6)$$

We estimated T_g as the mean temperature of the seven days leading up to each A_{net}/C_i curve, following that photosynthetic acclimation typically occurs along this timescale (e.g., as found in Smith and Dukes, 2018). Mean daily air temperature was estimated using data collected at a nearby weather station (station ID: USW000114762; coordinates: 40.355° N, 79.921° W) included in the Global Historical Climatology Network - Daily data product (Menne et al., 2012). V_{cmax25} and J_{max25} estimates were used to calculate the ratio of J_{max25} to V_{cmax25} (J_{max25}:V_{cmax25}; unitless) as an index of relative investment in electron transport for RuBP regeneration versus Rubisco carboxylation.

Stomatal limitation

The extent by which stomatal conductance limited net photosynthesis (unitless) was calculated following the approach described in Farquhar and Sharkey (1982), where:

$$Stomatal\ limitation = 1 - \frac{A_{net}}{A_{mod}} \quad (7)$$

A_{net} represents the measured net photosynthesis rate where atmospheric CO_2 is 420 μmol mol^{-1}. A_{mod} represents a theoretical photosynthetic rate where $C_i = C_a = 420$ μmol mol^{-1} (that is, no stomatal resistance to gas exchange), calculated as:

$$A_{mod} = V_{cmax}\frac{C_{i,mod} - \Gamma^*}{C_{i,mod} + K_m} - R_d \quad (8)$$

where V_{cmax} is the measured maximum rate of Rubisco carboxylation (i.e., not temperature-standardized to 25°C), $C_{i,mod}$ is the intercellular CO_2 concentration where $C_i = C_a$, set to 420 μmol mol^{-1}, Γ^* (μmol mol^{-1}) is the CO_2 compensation point in the absence of dark respiration, K_m is the Michaelis-Menten coefficient for Rubisco-limited photosynthesis (μmol mol^{-1}), and R_d is the dark respiration rate, estimated as a fixed proportion of V_{cmax}. K_m was calculated as:

$$K_m = K_c * \left(1 + \frac{O_i}{K_o}\right) \quad (9)$$

where K_c and K_o were calculated following Eqns. 1 and 2, respectively, while O_i is the leaf intercellular O_2 concentration, set to 210 μmol mol^{-1}.

Chlorophyll fluorescence measurements

Relative chlorophyll content was measured after each A_{net}/C_i curve on the same leaf using a Soil Plant Analysis Development chlorophyll meter (SPAD, unitless) built into the MultispeQ V2.0 handheld device (PhotosynQ Inc., East Lansing, MI, USA).

Soil characteristics

To characterize plant-available nitrogen and phosphorus at the time of leaf gas exchange measurements, resin strips (Membranes International Inc., Ringwood, NJ, USA) were placed approximately 10 cm below the soil surface to quantify mobile ammonium (ppm), nitrate (ppm), and phosphate (ppm) concentrations in each plot. An initial batch of resin strips was incubated in the field between April 19 and June 1, 2023, followed by a second batch inserted in the same plot location between May 30 and June 29, 2023. A total of 36 strips, 12 for each nutrient, were placed in each plot to account for the high degree of spatial heterogeneity of soil nutrient availability in temperate forests (Akana et al., 2023). Cation and anion concentrations were extracted from resin strips in 0.5 M potassium sulfate at a 1:5 dilution factor for ammonium, and nitrate, and 1 M HCl for phosphate. Concentrations of each nutrient were determined through end products of standard colorimetric reactions (D'Angelo et al., 2001; Doane & Horwáth, 2003; Lajtha et al., 1999; Weatherburn, 1967). Soil inorganic nitrogen availability was estimated as the sum of the ammonium and nitrate concentrations. The soil inorganic nitrogen-to-phosphorus ratio was estimated as the ratio of soil inorganic nitrogen availability to soil phosphate availability.

Soil moisture data were collected using TOMST® TMS-4 data loggers (TOMST® s.r.o., Prague, Czech Republic). One data logger was placed in each *A. petiolata* treatment of each plot (i.e., 2 data loggers per plot) on April 26, 2023 and recorded soil moisture pulses every 15 minutes. Volumetric soil moisture content (%) was calculated using the calibration curves for a silt loam soil reported in Wild et al. (2019). We calculated the mean daily volumetric soil moisture content and used these values as the primary indicator of soil moisture throughout the measurement period.

317 **Table 2** Replication statement for levels of inference used in this study

Measurement type	Scale of Inference	Scale at which the factor of interest is applied	Number of replicates at the appropriate scale
Soil nutrient availability	Plot	Plot (treatment is imposed in split-plot design)	3 plots x 6 resin strips per nutrient type per *A. petiolata* treatment per plot (12 resin strips per nutrient type per plot) = 18 replicates per nutrient type per *A. petiolata* treatment (36 total resin strips per nutrient across plots)
Soil moisture	Plot	Plot (treatment is imposed in split-plot design)	3 plots x 1 soil moisture sensor per *A. petiolata* treatment (2 soil moisture sensors per plot) = 3 replicates per *A. petiolata* treatment
Native plant photosynthetic traits	Species	7 photosynthetic traits per individual	4-20 individuals per species per *A. petiolata* treatment per plot. Total number of individuals per species: 33 *Trillium* spp. individuals, 32 *M. racemosum* individuals

318

319

Data analysis

We built a series of linear mixed-effects models to explore the effects of *A. petiolata* treatment and measurement period on soil nutrient availability. Each model included *A. petiolata* treatment (ambient, weeded) and measurement period (open, closed tree canopy) as fixed effects, with an additional interaction term between *A. petiolata* treatment and measurement period. Plot was included as a random intercept term. We constructed separate models with this independent variable structure for soil nitrate availability, soil ammonium availability, soil inorganic nitrogen (nitrate + ammonium) availability, soil phosphate availability, and the soil nitrogen-to-phosphorus ratio. The models for soil inorganic nitrogen availability and the soil nitrogen-to-phosphorus ratio were fitted using dependent variables that were natural-log transformed, while the model for soil ammonium availability was fitted after soil ammonium availability was square root-transformed to normalize model residuals (Shapiro-Wilk: $p>0.05$ in all cases).

Next, we built a linear mixed-effects model to explore the effect of *A. petiolata* treatment on volumetric soil moisture content across the measurement period. This model included *A. petiolata* treatment (ambient levels, weeded) and day of year (continuous) as fixed effects, with an added interaction term between *A. petiolata* treatment and day of year. Plot was included as a random intercept term.

Finally, we built a series of species-specific linear mixed-effects models to explore the effect of *A. petiolata* treatment and measurement period on leaf physiological traits of *Trillium* spp. and *M. racemosum*. Species were not concatenated into a single linear mixed-effect model for each trait because we did not seek to understand interspecies variability in measured traits. All models included *A. petiolata* treatment (ambient, weeded) and measurement period (open, closed tree canopy) as fixed effects, as well as an interaction term between *A. petiolata* treatment and measurement period. Plot was included as a random intercept term. Plant individual was also included as a random intercept term to account for repeated measures. Individuals were only included in analyses if gas exchange measurements were collected during both measurement periods. We constructed separate models with this independent variable structure for each species for the following dependent variables: A_{net}, g_{sw}, stomatal limitation, V_{cmax25}, J_{max25}, J_{max25}:V_{cmax25}, and SPAD. Models for A_{net}, g_{sw}, V_{cmax25}, and J_{max25} in *Trillium* spp. were fitted using dependent variables that were natural-log transformed to normalize model residuals, while models for stomatal limitation, *SPAD*, and J_{max25} in *M. racemosum* were fitted using dependent

variables that were natural-log transformed to normalize model residuals (Shapiro-Wilk: $p>0.05$ in all cases).

Each model was fitted using the 'lmer' function in the 'lme4' R package (Bates *et al.*, 2015). Type II Wald's χ^2 and the significance ($\alpha=0.05$) of each fixed effect coefficient was calculated using the 'Anova' function in the 'car' R package (Fox & Weisberg, 2019). We used the 'emmeans' R package (Lenth, 2019) to conduct post hoc comparisons using Tukey's tests, where degrees of freedom were approximated using the Kenward-Roger approach (Kenward & Roger, 1997). All analyses and plots were conducted in R version 4.1.0 (R Core Team, 2021). Data, analysis scripts, and plot scripts are available on Zenodo (DOI: 10.5281/13862911).

Results

Soil characteristics

Soil inorganic nitrogen availability was 69% lower ($p<0.001$, Table 3; Fig. 1a) and soil phosphate availability was 26% lower ($p=0.001$, Table 3; Fig. 1b) in samples collected after tree canopy closure compared to samples collected before tree canopy closure. This response led to a 188% decline in the soil nitrogen-to-phosphorus ratio ($p<0.001$, Table 3; Fig. 1c) after tree canopy closure. Soil nitrate availability was decreased by 71% in samples collected after the tree canopy closed ($p<0.001$, Table 3; Fig. S1), whereas soil ammonium availability did not change between measurement periods ($p=0.770$, Table 3; Fig. S1).

Alliaria petiolata treatment had no effect on soil inorganic nitrogen availability ($p=0.104$, Table 3; Fig. 1a), soil phosphate availability ($p=0.108$, Table 3; Fig. 1b), soil ammonium availability ($p=0.845$, Table 3; Fig. S1), or soil nitrate availability ($p=0.106$, Table 3; Fig. S1). However, the soil nitrogen-to-phosphorus ratio was marginally greater in the *A. petiolata*-ambient treatment compared to the *A. petiolata*-weeded treatment ($p=0.078$, Table 3; Fig. 1c) due to an insignificant 22% increase in soil inorganic nitrogen availability ($p=0.104$, Table 3) and insignificant 14% decrease in soil phosphate availability ($p=0.106$, Table 3; Fig. 1b) in the *A. petiolata*-ambient compared to the *A. petiolata*-weeded treatment.

Soil moisture decreased as the growth season progressed ($p<0.001$; Table 3; Fig. 1d) and was lower in the *A. petiolata*-ambient than the *A. petiolata*-weeded treatment ($p<0.001$; Table 3; Fig. 1d), with no interaction between *A. petiolata* treatment and day of year ($p=0.602$; Table 3; Fig. 1d).

382 **Table 3** Analysis of variance results exploring the role of *A. petiolata* treatment and
383 measurement period on soil nitrogen and phosphorus availability*

		A. petiolata treatment (A)		Canopy status (C) or day of year (D)		A×C or A×D	
	df	χ^2	*p*	χ^2	*p*	χ^2	*p*
Soil nitrogen availability	1	2.648	0.104	51.242	**<0.001**	2.438	0.118
Soil NO_3-N availability	1	2.609	0.106	63.730	**<0.001**	1.719	0.190
Soil NH_4-N availability	1	0.038	0.845	0.086	0.770	1.072	0.301
Soil phosphate availability	1	2.589	0.108	10.355	**0.001**	0.297	0.586
Soil N:P	1	3.115	*0.078*	24.827	**<0.001**	0.181	0.670
Soil moisture	1	17.778	**<0.001**	310.951	**<0.001**	0.272	0.602

384 *Significance determined using Type II Wald χ^2 tests (α=0.05). *P*-values less than 0.05 are in
385 bold, while $0.05<p<0.1$ are in italic font. Soil nutrient availabilities report results using *A.*
386 *petiolata* treatment, canopy status, and their interaction as fixed effects, while soil moisture
387 reports results using *A. petiolata* treatment, day of year, and their interaction as fixed effects.
388 Key: df = degrees of freedom

389 **Figure 1**

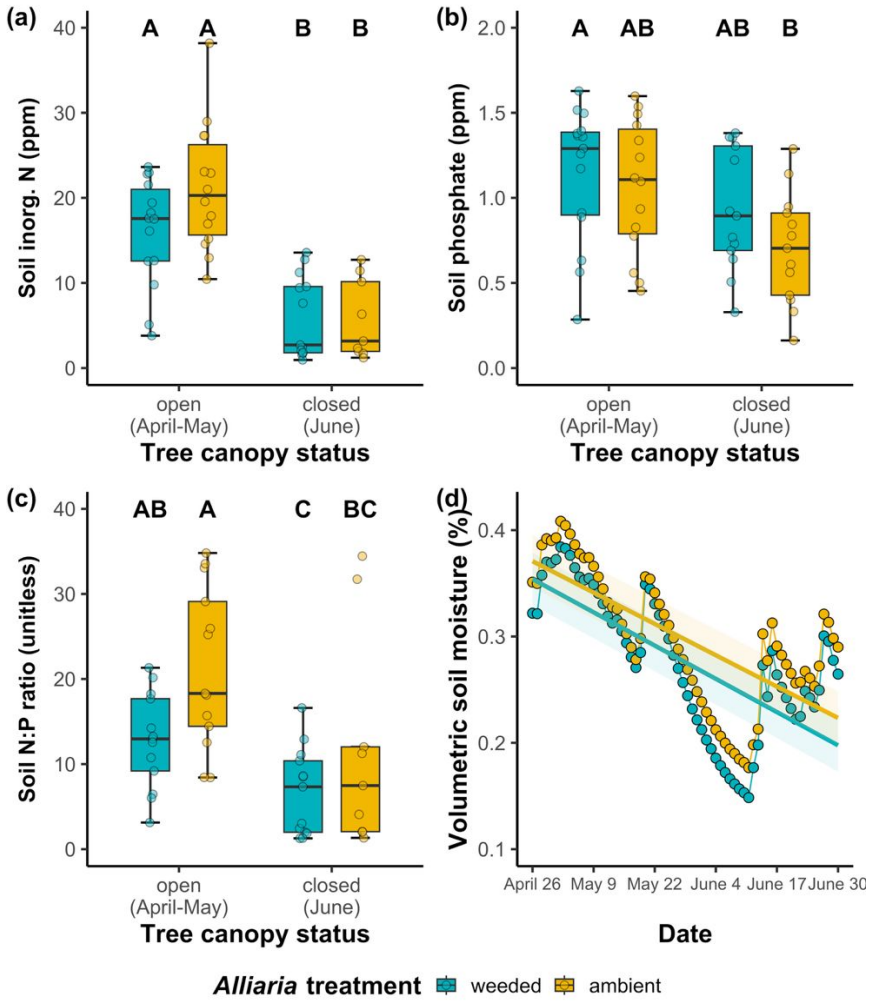

390

391 **Figure 1** Effects of *A. petiolata* treatment and measurement period on soil inorganic nitrogen
392 availability (a), soil phosphate availability (b), the soil nitrogen: phosphorus ratio (c), and
393 volumetric soil moisture (d). Tree canopy status is on the x-axis in panels a-c, while date is on
394 the x-axis in panel d. Teal points, boxplots, and trendlines indicate measurements collected in
395 plots where *A. petiolata* was weeded and gold points, boxplots, and trendlines indicate
396 measurements collected in subplots where *A. petiolata* was present at ambient levels. Boxes
397 represent the upper (75% percentile) and lower (25% percentile) quartiles, and whiskers
398 represent 1.5 times the upper and lower quartile values. Lettering above each treatment group
399 indicates statistically different groups where Tukey: $p<0.05$. In panel (d), each point references
400 daily volumetric soil water content averaged across the three plots used to collect gas exchange
401 measurements, and error ribbons represent the trendline standard error.

Gas exchange

For *Trillium* spp., net photosynthesis decreased by 64% (p<0.001, Table 4; Fig. 2a), stomatal conductance decreased by 20% (p<0.001, Table 4; Fig. 2c), and stomatal limitation decreased by 55% (p<0.001, Table 4; Fig. 2e) in measurements collected after tree canopy closure compared to before tree canopy closure. Net photosynthesis was marginally reduced in the *A. petiolata*-ambient treatment compared to the *A. petiolata*-weeded treatment (p=0.064, Table 4; Fig. 2a). This effect was driven by a 14% reduction in net photosynthesis in the *A. petiolata*-ambient treatment for measurements collected after canopy closure, as there was no treatment difference detected for measurements collected prior to tree canopy closure (*A. petiolata* treatment-by-canopy status interaction: p=0.032, Table 4; Fig. 2a). *Alliaria petiolata* treatment had no effect on stomatal conductance (p=0.726, Table 4; Fig. 2c) or stomatal limitation (p=0.751, Table 4; Fig. 2e).

For *M. racemosum*, net photosynthesis decreased by 59% (p<0.001, Table 4; Fig. 2b), stomatal conductance decreased by 63% (p<0.001, Table 4; Fig. 2d) and stomatal limitation increased by 14% (p<0.001, Table 4; Fig. 2f) in measurements collected after tree canopy closure compared to before tree canopy closure. In the *A. petiolata*-ambient treatment, net photosynthesis decreased by 12% (p=0.015, Table 4) and stomatal conductance decreased by 22% (p=0.002, Table 4), while stomatal limitation increased by 24% (p=0.007, Table 4) to the *A. petiolata*-weeded treatment. Despite no *A. petiolata*-by-canopy status interaction, net photosynthesis and stomatal conductance responses to *A. petiolata* were driven by significant treatment effects observed only after tree canopy closure (Tukey: p<0.05 in both cases; Fig. 2b, 2d). Stomatal limitation responses to *A. petiolata* were also driven by significant treatment effects that were only observed after tree canopy closure (*A. petiolata*-by-canopy status interaction: p=0.033; Table 4; Fig. 2f)

Relative chlorophyll content

SPAD values were 31% greater in *Trillium* spp. (p<0.001, Table 4; Fig. S2) and 47% greater in *M. racemosum* (p<0.001, Table 4; Fig. S2) in measurements collected after tree canopy closure compared to before tree canopy closure. *A. petiolata* treatment had no effect on SPAD in either species (p>0.05 in both cases, Table 4).

433 **Table 4** Analysis of variance results for the effects of *A. petiolata* treatment and measurement period on leaf gas exchange*

	A_{net}		g_{sw}		Stomatal limitation		*SPAD*	
	χ^2	*p*	χ^2	*p*	χ^2	*p*	χ^2	*p*
***Trillium* spp.**								
A. petiolata treatment (A)	3.439	*0.064*	0.123	0.726	0.101	0.751	0.061	0.805
Canopy status (C)	774.777	**<0.001**	12.969	**<0.001**	284.608	**<0.001**	77.290	**<0.001**
A×C	4.593	**0.032**	0.864	0.353	0.041	0.839	4.602	**0.032**
M. racemosum								
A. petiolata treatment (A)	5.932	**0.015**	9.515	**0.002**	7.208	**0.007**	1.486	0.223
Canopy status (C)	256.616	**<0.001**	137.246	**<0.001**	6.232	**0.013**	332.988	**<0.001**
A×C	0.298	0.585	0.199	0.655	4.534	**0.033**	2.338	0.126

434 *Significance determined using Type II Wald χ^2 tests (α=0.05). *P*-values less than 0.05 are in bold and 0.05<*p*<0.1 are in italics. Key:
435 A_{net} = light-saturated net photosynthesis rate (μmol m^{-2} s^{-1}), g_{sw} = stomatal conductance (mol m^{-2} s^{-1}), SPAD = relative chlorophyll
436 content (unitless)
437

438 **Figure 2**

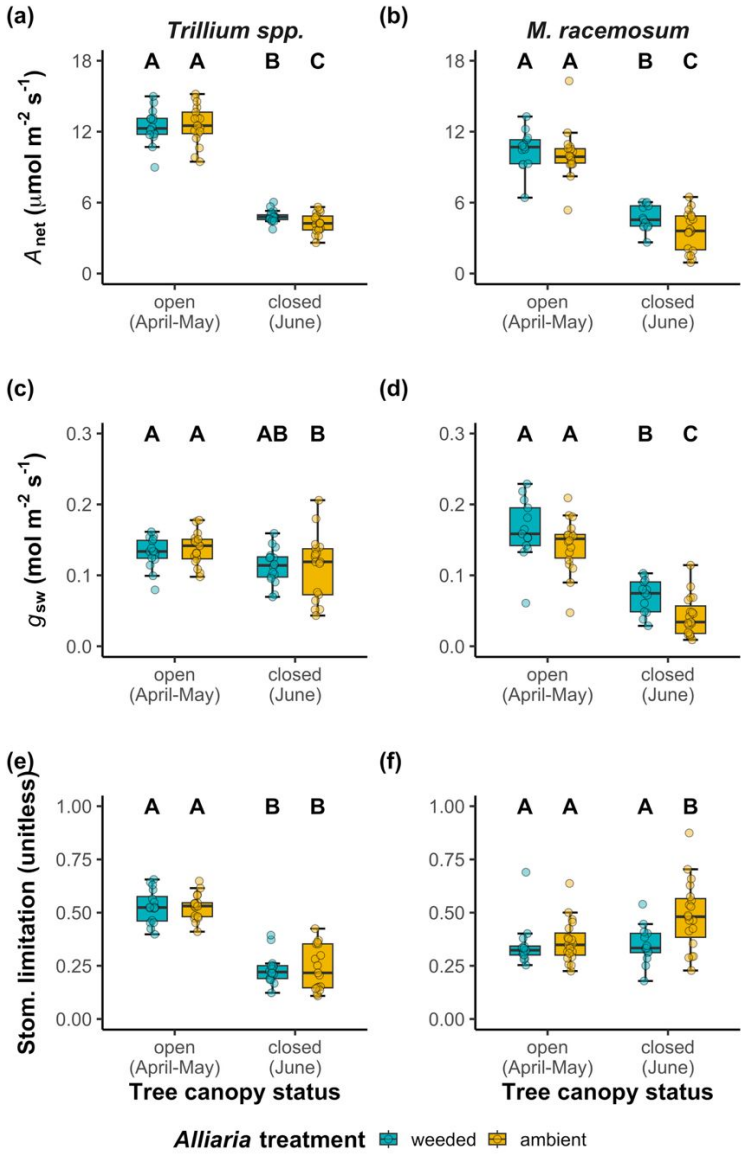

439

440 **Figure 2** Effects of *A. petiolata* treatment and tree canopy status on net photosynthesis (A_{net}, a-
441 b), stomatal conductance (g_{sw}, c-d), and stomatal limitation of net photosynthesis (e-f). The left
442 column shows *Trillium* spp. responses, while the right column shows *M. racemosum* responses.
443 Tree canopy status is on the x-axis. Teal points and boxplots indicate measurements collected in
444 plots where *A. petiolata* was weeded and gold points and boxplots indicate measurements
445 collected in plots where *A. petiolata* abundance was not manipulated. Boxes represent the upper
446 (75% percentile) and lower (25% percentile) quartiles, and whiskers represent 1.5 times the
447 upper and lower quartile values. Lettering above each treatment group indicates statistically
448 different groups where Tukey: $p<0.05$.

Photosynthetic capacity

In *Trillium* spp., V_{cmax25} decreased by 76% (p<0.001, Table 5; Fig. 3a) and J_{max25} decreased by 75% (p<0.001, Table 5; Fig. 3c) in measurements collected after tree canopy closure compared to before tree canopy closure. These patterns resulted in a 6% increase in J_{max25}:V_{cmax25} after tree canopy closure compared to before tree canopy closure (p=0.007; Table 5; Fig. 3e). In the *A. petiolata*-ambient treatment, V_{cmax25} was marginally reduced by 7% (p=0.100; Table 5; Fig. 3a) and J_{max25} was reduced by 10% (p=0.021; Table 5; Fig. 3c) compared to the *A. petiolata*-weeded treatment, leading to a 3% decrease in J_{max25}:V_{cmax25} (p=0.042; Table 5; Fig. 3e). The effects of *A. petiolata* treatment on V_{cmax25} and J_{max25} were due to significant treatment effects on both traits when measurements were collected after tree canopy closure, with no treatment effect detected for either of these traits prior to tree canopy closure (*A. petiolata* treatment-by-canopy status interaction: p<0.05 in both cases; Table 5; Fig. 3a, 3c).

For *M. racemosum*, V_{cmax25} decreased by 56% (p<0.001, Table 5; Fig. 3b) and J_{max25} decreased by 57% (p<0.001, Table 5; Fig. 3d) in measurements collected after tree canopy closure compared to measurements collected before tree canopy closure, while J_{max25}:V_{cmax25} did not change between the two measurement periods (p=0.335, Table 5; Fig. 3f). *Alliaria petiolata* treatment had no effect on V_{cmax25} (p=0.992, Table 5), J_{max25} (p=0.948, Table 5), or J_{max25}:V_{cmax25} (p=0.671, Table 5).

468 **Table 5** Analysis of variance results for the effects of *A. petiolata* treatment and measurement
469 period on apparent photosynthetic capacity*

	V_{cmax25}		J_{max25}		J_{max25}:V_{cmax25}	
	χ^2	*p*	χ^2	*p*	χ^2	*p*
***Trillium* spp.**						
A. petiolata treatment (A)	2.697	*0.100*	5.348	**0.021**	4.119	**0.042**
Canopy status (C)	1548.739	**<0.001**	1532.685	**<0.001**	11.226	**<0.001**
A×C	3.915	**0.048**	5.965	**0.015**	1.576	0.209
M. racemosum						
A. petiolata treatment (A)	<0.001	0.992	0.004	0.948	0.181	0.671
Canopy status (C)	260.475	**<0.001**	310.714	**<0.001**	0.928	0.335
A×C	0.417	0.519	0.006	0.937	2.070	0.150

470 *Significance determined using Type II Wald χ^2 tests (α=0.05). *P*-values less than 0.05 are in
471 bold and values where $0.05<p<0.1$ are italicized. Key: V_{cmax25} = maximum rate of Rubisco
472 carboxylation at 25°C (μmol m^{-2} s^{-1}), J_{max25} = maximum rate of electron transport for RuBP
473 regeneration at 25°C (μmol m^{-2} s^{-1}), J_{max25}:V_{cmax25} = ratio of J_{max25} to V_{cmax25} (unitless)
474

475 **Figure 3**

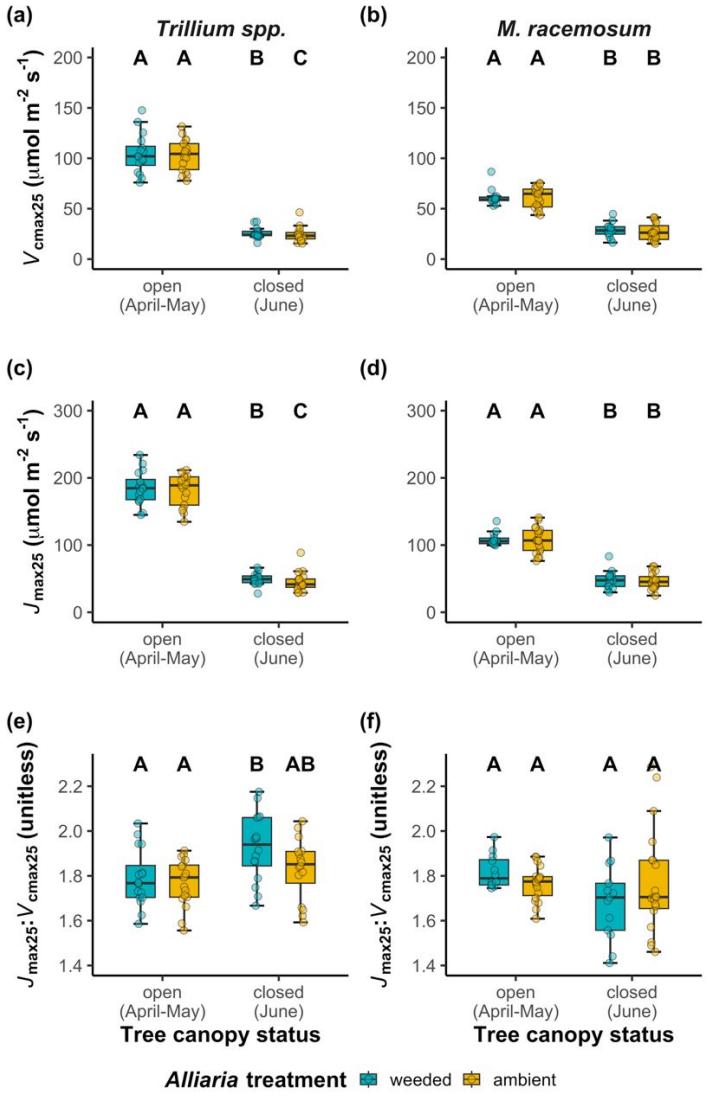

476

477 **Figure 3** Effects of *A. petiolata* treatment and tree canopy status on the temperature-standardized
478 maximum rate of Rubisco carboxylation (V_{cmax25}; a-b), the temperature-standardized maximum
479 rate of electron transport for RuBP regeneration (J_{max25}; c-d), and the ratio J_{max25}:V_{cmax25} (e-f).
480 The left column shows *Trillium* spp. responses, while the right column shows *M. racemosum*
481 responses. Tree canopy status is on the x-axis. Teal points and boxplots indicate measurements
482 collected in subplots where *A. petiolata* was weeded, and gold points and boxplots indicate
483 measurements collected in subplots where *A. petiolata* abundance was not manipulated. Boxes
484 represent the upper (75% percentile) and lower (25% percentile) quartiles, and whiskers
485 represent 1.5 times the upper and lower quartile values. Lettering above each treatment group
486 indicates statistically different groups where Tukey: $p<0.1$.

Discussion

Our results demonstrate that *A. petiolata* presence decreased net photosynthesis rates in both of the native understory species tested, but these patterns only became apparent after tree canopy closure. Reduced net photosynthesis rates in both species were affected by contrasting mechanisms: decreased apparent temperature-standardized photosynthetic capacity in *Trillium* spp. and reduced stomatal conductance in *M. racemosum*. Together, these findings highlight the need to understand species-specific responses to allelopathic invaders and other anthropogenic stressors to natural ecosystems, and to consider the temporal changes in the expression of native plant physiologies. In this system, these findings also provide a physiological mechanism that may help to understand how the effects of *A. petiolata* on AM fungal mutualism disruption could scale up to effect native plant population and community composition (Table 1).

Photosynthetic responses to A. petiolata presence are linked to altered nutrient and water economics

Both of the native species growing under ambient levels of *A. petiolata* exhibited significantly reduced net photosynthesis rates compared to those growing in the *A. petiolata*-weeded treatment, supporting our first hypothesis. In *Trillium* spp., this response was associated with a reduction in J_{max25}, a marginal reduction in V_{cmax25}, and no change in stomatal conductance or stomatal limitation. These patterns are indicative of increased photosynthetic nutrient stress and no apparent sign of water stress. In contrast, reduced net photosynthesis in *M. racemosum* was associated with a reduction in stomatal conductance, an increase in stomatal limitation, and no change in V_{cmax25} or J_{max25}. These patterns indicate that presence of the allelopathic invader induced water stress without signs of nutrient stress. Increased water stress in *M. racemosum* could reflect greater plot-level water demand in the *A. petiolata*-ambient treatment, where presence of *A. petiolata* may have increased plant density and thus community-level water uptake compared to weeded plots. However, *Trillium* spp. did not exhibit these water stress signatures, and similar net photosynthesis and stomatal conductance patterns were observed in a controlled greenhouse experiment under well-watered conditions (Hale et al., 2016). These patterns corresponded with null effects of *A. petiolata* treatment on apparent photosynthetic capacity, consistent with previous work showing that *M. racemosum* responses to *A. petiolata* invasion are associated with changes in water, not nutrient, economics (Hale et al., 2011, 2016).

Contrasting mechanisms that defined the physiological responses of *Trillium* spp. and *M. racemosum* to *A. petiolata* may be explained through the lens of the leaf economics spectrum (Reich, 2014; Wright et al., 2004). While *Trillium* spp. and *M. racemosum* share many functional and ecological traits, such as rhizome formation, clonal reproduction, nutrient and water acquisition through direct uptake pathways or symbioses with AM fungi, and similar spring emergence times (Brundrett & Kendrick, 1987, 1990; Heberling et al., 2019), these two species differ in leaf lifespan (Heberling et al., 2019), placing them at different positions along the leaf economics spectrum (Onoda et al., 2017; Reich, 2014; Wright et al., 2004). Relatively short-lived *Trillium* spp. leaves require rapid nutrient uptake to support faster growth and reproduction, whereas longer-lived *M. racemosum* leaves may adopt resource-conservative strategies that depend on sustained water use. Consistent with this hypothesis, *M. racemosum* exhibited lower V_{cmax25} on average than *Trillium* (V_{cmax25} mean ± SD: 44.4 ± 19.1 μmol m^{-2} s^{-1} in *M. racemosum*, 65.3 ± 41.8 μmol m^{-2} s^{-1} in *Trillium* spp.), reflecting its more conservative strategy. Tracer studies that quantify nutrient and water usage at the leaf-level may be needed to verify whether this is the case.

Photosynthetic responses to A. petiolata presence are only observed after tree canopy closure

Contrary to our second hypothesis, *A. petiolata* treatment effects were absent early in the season when understory demand for soil resources was presumed to be the greatest. This null response may be attributed to resource optimization that caused individuals in both treatments to favor investment toward direct uptake. Resource optimization theory predicts that, given multiple potential acquisition strategies (e.g., direct uptake, mycorrhizal symbioses, etc.), plants should prioritize investment toward the resource uptake strategy that minimizes the cost and maximizes the uptake efficiency of acquiring soil resources (Bloom et al., 1985; Kummel & Salant, 2006; Rastetter et al., 2001). Thus, plants should invest more strongly in direct uptake pathways early in the growing season when soil resources are more abundant, as costs to acquire soil resources through direct uptake pathways are often reduced under high resource availability (Lu et al., 2022; Perkowski et al., 2021, 2024). Null photosynthetic responses early in the growing season may have been due to investment toward direct uptake that allowed individuals to satisfy demand to build and maintain photosynthetic enzymes and maintain transpiration while minimizing any negative consequence of relying on disrupted AM fungal partners for resources.

549 Supporting our second hypothesis, the effects of *A. petiolata* treatment on leaf-level
550 photosynthetic traits were only observed after tree canopy closure. This pattern was associated
551 with decreased nitrogen availability, phosphorus availability, and soil moisture following tree
552 canopy closure. These patterns suggest that late-season photosynthetic responses to *A. petiolata*
553 treatment may have been due to increased reliance on disrupted AM fungal partners as the cost to
554 acquire resources through direct uptake increased with reduced nutrient and water availability
555 (Perkowski et al., 2021, 2024). This may have been further exacerbated by a reduction in soil
556 moisture in the *A. petiolata*-ambient treatment and may have also been indicative of increased
557 phosphorus limitation. It is important to note that this study cannot separate the effects of canopy
558 closure from effects on soil resource availability. Additionally, we did not explicitly assess the
559 link between AM fungal mutualism disruption and native plant physiology responses to *A.*
560 *petiolata*, which is an important next step toward understanding how soil microbial community
561 disruption due to allelopathic invaders scale to impact native plant physiology and community
562 composition. Specifically, isotopic tracers (e.g., Hodge & Fitter, 2010) or soil resource
563 manipulation experiments across different AM fungal communities (e.g., Gustafson & Casper,
564 2004) would be a useful next step for linking soil microbial community, soil resource
565 availability, and photosynthetic responses of native species to allelopathic invaders.
566 Overall, these findings highlight the necessity of quantifying the temporal effects of plant
567 invasion on coexisting native plant populations. Ecophysiological studies have traditionally
568 focused on the impacts of allelopathic invaders on the physiological processes of native species
569 at single timepoints. While results from that approach provide a snapshot of plant invader effects
570 on native populations' physiology, assuming that they represent native physiology across the
571 growing season can be misleading. This risk may be especially important in systems where light
572 availability is a function of tree canopy closure and soil resource availability declines across the
573 growing season. Experiments that assess the impacts of plant invasion across more than one
574 timepoint, as reported here, can provide important insight into physiological mechanisms that
575 underpin the effects of plant invasion on native populations. Further, they provide important
576 empirical data that improves our ability to reliably predict how plant invasion scales up to plant
577 population and community dynamics. Finally, soil microbial and plant communities operate on
578 largely different spatiotemporal scales, which poses a challenge when scaling soil microbial
579 community changes up to plant community dynamics. Quantifying differential physiological

responses across the growing season by coexisting native plant species in the context of community invasion may allow us to integrate and scale the effects of plant invasions on belowground soil microbial and plant community dynamics.

Using leaf physiology to assess linkages between aboveground and belowground responses to allelopathic plant invasion

Native species' physiological responses to *A. petiolata* treatments have direct implications for understanding the integrated negative effects of *A. petiolata* invasion on the belowground soil microbial community and aboveground plant community form and function. *Alliaria petiolata* disrupts the belowground AM fungal community composition by reducing AM fungal biomass and root colonization rates while also increasing AM fungal richness (Table 1; Anthony et al., 2019; Bialic-Murphy et al., 2021; Burke, 2008; Burke et al., 2011, 2019; Cantor et al., 2011; Roche et al., 2021). This allelopathic invader also negatively affects the abundance and survivorship of AM native plants that coexist with *A. petiolata* in its non-native range (Bialic-Murphy et al., 2020; Callaway et al., 2008; Roche et al., 2021, 2023). Our results indicate that photosynthetic responses to *A. petiolata* are directionally similar to its impacts on AM fungal community and plant community dynamics (Table 1), suggesting that the effects of *A. petiolata* invasion may be inherently scalable through its impacts on native plant physiology.

References

Akana, P. R., Mifsud, I. E. J., & Menge, D. N. L. (2023). Soil nitrogen availability in a temperate forest exhibits large variability at sub-tree spatial scales. *Biogeochemistry*, *164*(3), 537–553. https://doi.org/10.1007/s10533-023-01056-5

Ali, A. A., Xu, C., Rogers, A., McDowell, N. G., Medlyn, B. E., Fisher, R. A., Wullschleger, S. D., Reich, P. B., Vrugt, J. A., Bauerle, W. L., Santiago, L. S., & Wilson, C. J. (2015). Global-scale environmental control of plant photosynthetic capacity. *Ecological Applications*, *25*(8), 2349–2365. https://doi.org/10.1890/14-2111.1

Anthony, M. A., Stinson, K. A., Trautwig, A. N., Coates-Connor, E., & Frey, S. D. (2019). Fungal communities do not recover after removing invasive *Alliaria petiolata* (garlic mustard). *Biological Invasions*, *21*(10), 3085–3099. https://doi.org/10.1007/s10530-019-02031-8

611 Atkin, O. K., & Tjoelker, M. G. (2003). Thermal acclimation and the dynamic response of plant
612 respiration to temperature. *Trends in Plant Science*, *8*(7), 343–351.
613 https://doi.org/10.1016/S1360-1385(03)00136-5
614 Bernacchi, C. J., Singsaas, E. L., Pimentel, C., Portis, A. R., & Long, S. P. (2001). Improved
615 temperature response functions for models of Rubisco-limited photosynthesis. *Plant, Cell*
616 *and Environment*, *24*(2), 253–259. https://doi.org/10.1046/j.1365-3040.2001.00668.x
617 Bialic-Murphy, L., Brouwer, N. L., & Kalisz, S. (2020). Direct effects of a non-native invader
618 erode native plant fitness in the forest understory. *Journal of Ecology*, *108*(1), 189–198.
619 https://doi.org/10.1111/1365-2745.13233
620 Bialic-Murphy, L., Smith, N. G., Voothuluru, P., McElderry, R. M., Roche, M. D., Cassidy, S.
621 T., Kivlin, S. N., & Kalisz, S. (2021). Invasion-induced root–fungal disruptions alter plant
622 water and nitrogen economies. *Ecology Letters*, *24*(6), 1145–1156.
623 https://doi.org/10.1111/ele.13724
624 Bloom, A. J., Chapin, F. S., & Mooney, H. A. (1985). Resource limitation in plants-an economic
625 analogy. *Annual Review of Ecology and Systematics*, *16*(1), 363–392.
626 https://doi.org/10.1146/annurev.es.16.110185.002051
627 Brouwer, N. L., Hale, A. N., & Kalisz, S. (2015). Mutualism-disrupting allelopathic invader
628 drives carbon stress and vital rate decline in a forest perennial herb. *AoB PLANTS*, *7*(1), 1–
629 14. https://doi.org/10.1093/aobpla/plv014
630 Brundrett, M. C., & Kendrick, B. (1987). The mycorrhizal status, root anatomy, and phenology
631 of plants in a sugar maple forest. *Canadian Journal of Botany*, *66*, 1153–1173.
632 Brundrett, M. C., & Kendrick, B. (1990). The roots and mycorrhizas of herbaceous woodland
633 plants: I. Quantitative aspects of morphology. *New Phytologist*, *114*(3), 457–468.
634 https://doi.org/10.1111/j.1469-8137.1990.tb00415.x
635 Burke, D. J. (2008). Effects of *Alliaria petiolata* (garlic mustard; Brassicaceae) on mycorrhizal
636 colonization and community structure in three herbaceous plants in a mixed deciduous
637 forest. *American Journal of Botany*, *95*(11), 1416–1425.
638 https://doi.org/10.3732/ajb.0800184
639 Burke, D. J., Carrino-Kyker, S. R., Hoke, A., Cassidy, S., Bialic-Murphy, L., & Kalisz, S.
640 (2019). Deer and invasive plant removal alters mycorrhizal fungal communities and soil

641 chemistry: Evidence from a long-term field experiment. *Soil Biology and Biochemistry*,
642 *128*(September 2018), 13–21. https://doi.org/10.1016/j.soilbio.2018.09.031
643 Burke, D. J., Weintraub, M. N., Hewins, C. R., & Kalisz, S. (2011). Relationship between soil
644 enzyme activities, nutrient cycling and soil fungal communities in a northern hardwood
645 forest. *Soil Biology and Biochemistry*, *43*(4), 795–803.
646 https://doi.org/10.1016/j.soilbio.2010.12.014
647 Callaway, R. M., Cipollini, D., Barto, K., Thelen, G. C., Hallett, S. G., Prati, D., Stinson, K., &
648 Klironomos, J. (2008). Novel weapons: Invasive plant suppresses fungal mutualists in
649 America but not in its native Europe. *Ecology*, *89*(4), 1043–1055.
650 https://doi.org/10.1890/07-0370.1
651 Callaway, R. M., & Ridenour, W. M. (2004). Novel weapons: Invasive success and the evolution
652 of increased competitive ability. *Frontiers in Ecology and the Environment*, *2*(8), 436–443.
653 https://doi.org/10.1890/1540-9295(2004)002[0436:NWISAT]2.0.CO;2
654 Cantor, A., Hale, A., Aaron, J., Traw, M. B., & Kalisz, S. (2011). Low allelochemical
655 concentrations detected in garlic mustard-invaded forest soils inhibit fungal growth and
656 AMF spore germination. *Biological Invasions*, *13*(12), 3015–3025.
657 https://doi.org/10.1007/s10530-011-9986-x
658 D'Angelo, E., Crutchfield, J., & Vandiviere, M. (2001). Rapid, sensitive, microscale
659 determination of phosphate in water and soil. *Journal of Environmental Quality*, *30*(6),
660 2206–2209. https://doi.org/10.2134/jeq2001.2206
661 Doane, T. A., & Horwáth, W. R. (2003). Spectrophotometric determination of nitrate with a
662 single reagent. *Analytical Letters*, *36*(12), 2713–2722. https://doi.org/10.1081/AL-
663 120024647
664 Duursma, R. A. (2015). Plantecophys - an R package for analysing and modelling leaf gas
665 exchange data. *PLOS ONE*, *10*(11), e0143346.
666 https://doi.org/10.1371/journal.pone.0143346
667 Ellsworth, D. S., Crous, K. Y., De Kauwe, M. G., Verryckt, L. T., Goll, D., Zaehle, S.,
668 Bloomfield, K. J., Ciais, P., Cernusak, L. A., Domingues, T. F., Dusenge, M. E., Garcia, S.,
669 Guerrieri, R., Ishida, F. Y., Janssens, I. A., Kenzo, T., Ichie, T., Medlyn, B. E., Meir, P., …
670 Wright, I. J. (2022). Convergence in phosphorus constraints to photosynthesis in forests

around the world. *Nature Communications*, *13*(1), 5005. https://doi.org/10.1038/s41467-022-32545-0

Evans, J. R. (1989). Photosynthesis and nitrogen relationships in leaves of C_3 plants. *Oecologia*, *78*(1), 9–19. https://doi.org/10.1007/BF00377192

Evans, J. R., & Clarke, V. C. (2019). The nitrogen cost of photosynthesis. *Journal of Experimental Botany*, *70*(1), 7–15. https://doi.org/10.1093/jxb/ery366

Evans, J. R., & Seemann, J. R. (1989). The allocation of protein nitrogen in the photosynthetic apparatus: costs, consequences, and control. *Photosynthesis*, *8*, 183–205.

Farquhar, G. D., & Sharkey, T. D. (1982). Stomatal conductance and photosynthesis. *Annual Review of Plant Physiology*, *33*(1), 317–345. https://doi.org/10.1146/annurev.pp.33.060182.001533

Farquhar, G. D., von Caemmerer, S., & Berry, J. A. (1980). A biochemical model of photosynthetic CO_2 assimilation in leaves of C_3 species. *Planta*, *149*(1), 78–90. https://doi.org/10.1007/BF00386231

Fox, J., & Weisberg, S. (2019). *An R companion to applied regression* (Third edit). Sage. https://socialsciences.mcmaster.ca/jfox/Books/Companion/

Gustafson, D. J., & Casper, B. B. (2004). Nutrient addition affects AM fungal performance and expression of plant/fungal feedback in three serpentine grasses. *Plant and Soil*, *259*(1–2), 9–17. https://doi.org/10.1023/B:PLSO.0000020936.56786.a4

Hale, A. N., & Kalisz, S. (2012). Perspectives on allelopathic disruption of plant mutualisms: A framework for individual- and population-level fitness consequences. *Plant Ecology*, *213*(12), 1991–2006. https://doi.org/10.1007/s11258-012-0128-z

Hale, A. N., Lapointe, L., & Kalisz, S. (2016). Invader disruption of belowground plant mutualisms reduces carbon acquisition and alters allocation patterns in a native forest herb. *New Phytologist*, *209*(2), 542–549. https://doi.org/10.1111/nph.13709

Hale, A. N., Tonsor, S. J., & Kalisz, S. (2011). Testing the mutualism disruption hypothesis: physiological mechanisms for invasion of intact perennial plant communities. *Ecosphere*, *2*(10), art110. https://doi.org/10.1890/es11-00136.1

Heberling, J. M., Cassidy, S. T., Fridley, J. D., & Kalisz, S. (2019). Carbon gain phenologies of spring-flowering perennials in a deciduous forest indicate a novel niche for a widespread invader. *New Phytologist*, *221*(2), 778–788. https://doi.org/10.1111/nph.15404

Hodge, A., & Fitter, A. H. (2010). Substantial nitrogen acquisition by arbuscular mycorrhizal fungi from organic material has implications for N cycling. *Proceedings of the National Academy of Sciences*, *107*(31), 13754–13759.

Hungate, B. A., Dukes, J. S., Shaw, M. R., Luo, Y., & Field, C. B. (2003). Nitrogen and climate change. *Science*, *302*(5650), 1512–1513. https://doi.org/10.1126/science.1091390

Inderjit, Wardle, D. A., Karban, R., & Callaway, R. M. (2011). The ecosystem and evolutionary contexts of allelopathy. *Trends in Ecology and Evolution*, *26*(12), 655–662. https://doi.org/10.1016/j.tree.2011.08.003

Kalisz, S., Kivlin, S. N., & Bialic-Murphy, L. (2021). Allelopathy is pervasive in invasive plants. *Biological Invasions*, *23*(2), 367–371. https://doi.org/10.1007/s10530-020-02383-6

Kattge, J., & Knorr, W. (2007). Temperature acclimation in a biochemical model of photosynthesis: a reanalysis of data from 36 species. *Plant, Cell & Environment*, *30*(9), 1176–1190. https://doi.org/10.1111/j.1365-3040.2007.01690.x

Kenward, M. G., & Roger, J. H. (1997). Small sample inference for fixed effects from restricted maximum likelihood. *Biometrics*, *53*(3), 983. https://doi.org/10.2307/2533558

Kummel, M., & Salant, S. W. (2006). The economics of mutualisms: Optimal utilization of mycorrhizal mutualistic partners by plants. *Ecology*, *87*(4), 892–902. https://doi.org/10.1890/0012-9658(2006)87[892:TEOMOU]2.0.CO;2

Lajtha, K., Driscoll, C. T., Jarrell, W. M., & Elliott, E. T. (1999). Soil phosphorus. In *Standard Soil Methods for Long-Term Ecological Research* (p. 115).

Lenth, R. (2019). *emmeans: estimated marginal means, aka least-squares means*. https://cran.r-project.org/package=emmeans

Lu, J., Yang, J., Keitel, C., Yin, L., Wang, P., Cheng, W., & Dijkstra, F. A. (2022). Belowground carbon efficiency for nitrogen and phosphorus acquisition varies between *Lolium perenne* and *Trifolium repens* and depends on phosphorus fertilization. *Frontiers in Plant Science*, *13*, 1–9. https://doi.org/10.3389/fpls.2022.927435

Medlyn, B. E., Dreyer, E., Ellsworth, D. S., Forstreuter, M., Harley, P. C., Kirschbaum, M. U. F., Le Roux, X., Montpied, P., Strassemeyer, J., Walcroft, A., Wang, K., & Loustau, D. (2002). Temperature response of parameters of a biochemically based model of photosynthesis. II. A review of experimental data. *Plant, Cell & Environment*, *25*(9), 1167–1179. https://doi.org/10.1046/j.1365-3040.2002.00891.x

Medrano, H., Escalona, J. M., Bota, J., Gulías, J., & Flexas, J. (2002). Regulation of Photosynthesis of C3 Plants in Response to Progressive Drought: Stomatal Conductance as a Reference Parameter. *Annals of Botany*, *89*(7), 895–905. https://doi.org/10.1093/aob/mcf079

Menne, M. J., Durre, I., Vose, R. S., Gleason, B. E., & Houston, T. G. (2012). An overview of the global historical climatology network-daily database. *Journal of Atmospheric and Oceanic Technology*, *29*(7), 897–910. https://doi.org/10.1175/JTECH-D-11-00103.1

Mutz, J., Heberling, J. M., Kivlin, S. N., Smith, N. G., Chatterjee, S., Perkowski, E. A., Bialic-Murphy, L., & Kalisz, S. (n.d.). *Allelopathic invader alters belowground plant-fungal interactions, physiology, and biomass allocation in native understory species*.

Onoda, Y., Wright, I. J., Evans, J. R., Hikosaka, K., Kitajima, K., Niinemets, Ü., Poorter, H., Tosens, T., & Westoby, M. (2017). Physiological and structural tradeoffs underlying the leaf economics spectrum. *New Phytologist*, *214*(4), 1447–1463. https://doi.org/10.1111/nph.14496

Palecki, M., Durre, I., Applequist, S., Arguez, A., & Lawrimore, J. H. (2021). U.S. Climate Normals 2020: U.S. Hourly Climate Normals (1991-2020). *NOAA National Centers for Environmental Information*.

Perkowski, E. A., Ezekannagha, E., & Smith, N. G. (2025). Nitrogen demand, availability, and acquisition strategy control plant responses to elevated CO_2. *Journal of Experimental Botany*, *76*(10), 2908–2923. https://doi.org/10.1093/jxb/eraf118

Perkowski, E. A., Terrones, J., German, H. L., & Smith, N. G. (2024). Symbiotic nitrogen fixation reduces belowground biomass carbon costs of nitrogen acquisition under low, but not high, nitrogen availability. *AoB PLANTS*, *16*(5), 1–22. https://doi.org/10.1093/aobpla/plae051

Perkowski, E. A., Waring, E. F., & Smith, N. G. (2021). Root mass carbon costs to acquire nitrogen are determined by nitrogen and light availability in two species with different nitrogen acquisition strategies. *Journal of Experimental Botany*, *72*(15), 5766–5776. https://doi.org/10.1093/jxb/erab253

Qu, T., Du, X., Peng, Y., Guo, W., Zhao, C., & Losapio, G. (2021). Invasive species allelopathy decreases plant growth and soil microbial activity. *PLoS ONE*, *16*(2 February), 1–12. https://doi.org/10.1371/journal.pone.0246685

764 R Core Team. (2021). *R: A language and environment for statistical computing* (4.1.1). R
765 Foundation for Statistical Computing. https://www.r-project.org/
766 Rastetter, E. B., Vitousek, P. M., Field, C. B., Shaver, G. R., Herbert, D., & Ågren, G. I. (2001).
767 Resource optimization and symbiotic nitrogen fixation. *Ecosystems*, *4*(4), 369–388.
768 https://doi.org/10.1007/s10021-001-0018-z
769 Reich, P. B. (2014). The world-wide 'fast-slow' plant economics spectrum: a traits manifesto.
770 *Journal of Ecology*, *102*(2), 275–301. https://doi.org/10.1111/1365-2745.12211
771 Roche, M. D., Pearse, I. S., Bialic-Murphy, L., Kivlin, S. N., Sofaer, H. R., & Kalisz, S. (2021).
772 Negative effects of an allelopathic invader on AM fungal plant species drive community-
773 level responses. *Ecology*, *102*(1), 1–12. https://doi.org/10.1002/ecy.3201
774 Roche, M. D., Pearse, I. S., Sofaer, H. R., Kivlin, S. N., Spyreas, G., Zaya, D. N., & Kalisz, S.
775 (2023). Invasion-mediated mutualism disruption is evident across heterogeneous
776 environmental conditions and varying invasion intensities. *Ecography*, *2023*(7), 1–11.
777 https://doi.org/10.1111/ecog.06434
778 Rodgers, V. L., Stinson, K. A., & Finzi, A. C. (2008). Ready or not, garlic mustard is moving in:
779 *Alliaria petiolata* as a member of eastern north American forests. *BioScience*, *58*(5), 426–
780 436. https://doi.org/10.1641/B580510
781 Saathoff, A. J., & Welles, J. (2021). Gas exchange measurements in the unsteady state. *Plant*
782 *Cell and Environment*, *44*(11), 3509–3523. https://doi.org/10.1111/pce.14178
783 Smith, N. G., & Dukes, J. S. (2018). Drivers of leaf carbon exchange capacity across biomes at
784 the continental scale. *Ecology*, *99*(7), 1610–1620. https://doi.org/10.1002/ecy.2370
785 Smith, S. E., & Read, D. J. (2008). *Mycorrhizal Symbiosis*.
786 Tejera-Nieves, M., Seong, D. Y., Reist, L., & Walker, B. J. (2024). The Dynamic Assimilation
787 Technique measures photosynthetic CO_2 response curves with similar fidelity to steady-
788 state approaches in half the time. *Journal of Experimental Botany*, *75*(10), 2819–2828.
789 https://doi.org/10.1093/jxb/erae057
790 USDA NRCS. (2022). The PLANTS Database. *(Http://Plants.Usda.Gov, 18 November 2022).*
791 *National Plant Data Team, Greensboro, NC 27401-4901 USA.*
792 Walker, A. P., Beckerman, A. P., Gu, L., Kattge, J., Cernusak, L. A., Domingues, T. F., Scales,
793 J. C., Wohlfahrt, G., Wullschleger, S. D., & Woodward, F. I. (2014). The relationship of
794 leaf photosynthetic traits - V_{cmax} and J_{max} - to leaf nitrogen, leaf phosphorus, and specific

leaf area: a meta-analysis and modeling study. *Ecology and Evolution*, *4*(16), 3218–3235. https://doi.org/10.1002/ece3.1173

Waring, E. F., Perkowski, E. A., & Smith, N. G. (2023). Soil nitrogen fertilization reduces relative leaf nitrogen allocation to photosynthesis. *Journal of Experimental Botany*, *74*(17), 5166–5180. https://doi.org/10.1093/jxb/erad195

Weatherburn, M. W. (1967). Phenol-hypochlorite reaction for determination of ammonia. *Analytical Chemistry*, *39*(8), 971–974. https://doi.org/10.1021/ac60252a045

Wild, J., Kopecký, M., Macek, M., Šanda, M., Jankovec, J., & Haase, T. (2019). Climate at ecologically relevant scales: A new temperature and soil moisture logger for long-term microclimate measurement. *Agricultural and Forest Meteorology*, *268*(July 2018), 40–47. https://doi.org/10.1016/j.agrformet.2018.12.018

Wright, I. J., Reich, P. B., Westoby, M., Ackerly, D. D., Baruch, Z., Bongers, F., Cavender-Bares, J., Chapin, T., Cornelissen, J. H. C., Diemer, M., Flexas, J., Garnier, E., Groom, P. K., Gulias, J., Hikosaka, K., Lamont, B. B., Lee, T. D., Lee, W., Lusk, C. H., … Villar, R. (2004). The worldwide leaf economics spectrum. *Nature*, *428*(6985), 821–827. https://doi.org/10.1038/nature02403

Zhang, Z., Liu, Y., Yuan, L., Weber, E., & van Kleunen, M. (2021). Effect of allelopathy on plant performance: a meta-analysis. *Ecology Letters*, *24*(2), 348–362. https://doi.org/10.1111/ele.13627

Supporting Information

Figure S1 Effects of *A. petiolata* treatment and tree canopy status on soil nitrate and ammonium availability

Figure S2 Effects of *A. petiolata* treatment and tree canopy status on relative chlorophyll content in *Trillium* spp. and *M. racemosum*.